

Organic & Biomolecular Chemistry

Accepted Manuscript



This is an *Accepted Manuscript*, which has been through the Royal Society of Chemistry peer review process and has been accepted for publication.

Accepted Manuscripts are published online shortly after acceptance, before technical editing, formatting and proof reading. Using this free service, authors can make their results available to the community, in citable form, before we publish the edited article. We will replace this *Accepted Manuscript* with the edited and formatted *Advance Article* as soon as it is available.

You can find more information about *Accepted Manuscripts* in the [Information for Authors](#).

Please note that technical editing may introduce minor changes to the text and/or graphics, which may alter content. The journal's standard [Terms & Conditions](#) and the [Ethical guidelines](#) still apply. In no event shall the Royal Society of Chemistry be held responsible for any errors or omissions in this *Accepted Manuscript* or any consequences arising from the use of any information it contains.

ARTICLE

Mitochondria-targeted turn-on fluorescent probe based on a rhodol platform for the detection of copper(I)

Cite this: DOI: 10.1039/x0xx00000x

Masayasu Taki,^{*a,b} Kazushi Akaoka,^b Koji Mitsui^b and Yukio Yamamoto^bReceived 00th January 2012,
Accepted 00th January 2012

DOI: 10.1039/x0xx00000x

www.rsc.org/

A new spirocyclized rhodol-based fluorescent probe has been developed for detecting mitochondrial Cu^+ . Alkylation of the hydroxy group of xanthen moiety with a tris(2-pyridylmethyl)amine-based ligand induced the formation of a non-fluorescent spirocyclic structure. The reaction with Cu^+ in the presence of submillimolar concentrations of glutathione at physiological pH resulted in the elimination of the ligand together with an increase in the fluorescence of the rhodol fluorophore. This probe was used to visualize mitochondrial Cu^+ in copper supplemented cells.

Introduction

Mitochondria are membrane-bound organelles that account for as much as 20% of the total cell volume. The main function of the mitochondrion is the generation of ATP via the respiratory reduction of oxygen to water with the simultaneous oxidation of NADH and FADH_2 . Copper is an essential cofactor within the mitochondrial matrices of cytochrome c oxidase (CcO) and superoxide dismutase (SOD1) enzymes, which play critical roles in the production of cellular energy and the execution of apoptotic events, respectively.¹ In contrast, copper is also potentially toxic because of its chemical redox potential and ability to produce hydroxyl radicals via the Fenton reaction. The uptake, efflux, and subcellular distribution of copper are therefore strictly regulated through a system of protein transporters and copper-chaperones.² Within the mitochondrial intermembrane space (IMS), CcO and SOD are metallated by pathways consisting of several IMS copper metallochaperones, such as COX17 and CCS, which are supplied with Cu^+ by a small copper-ligand complex in the mitochondrial matrix (MM).³ The basic biological knowledge of copper concentrations within the IMS and MM, however, as well as the general level of understanding of the mechanisms underlying mitochondrial copper homeostasis remains poor.

Fluorescent probes that can effectively visualize the distribution of copper within discrete subcellular organelles represent powerful tools for investigating copper homeostasis at the cellular level.⁴ Chang et al. reported a mitochondria-targeted fluorescent probe for Cu^+ (Mito-CS1) based on a photo-induced electron transfer mechanism.⁵ This probe contained a cationic triphenylphosphonium (TPP) group that selectively accumulated in the mitochondria and allowed for

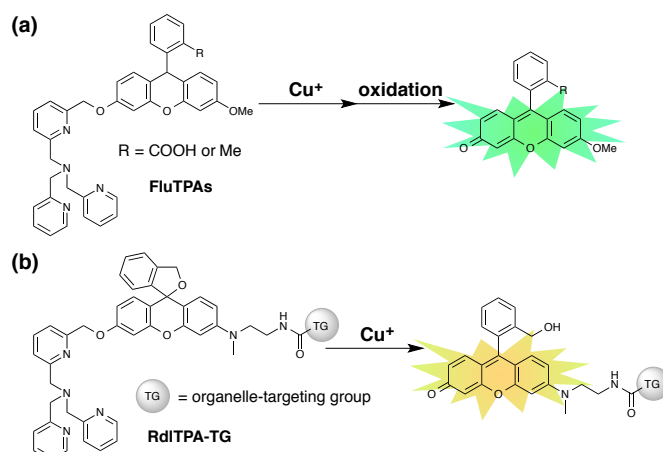
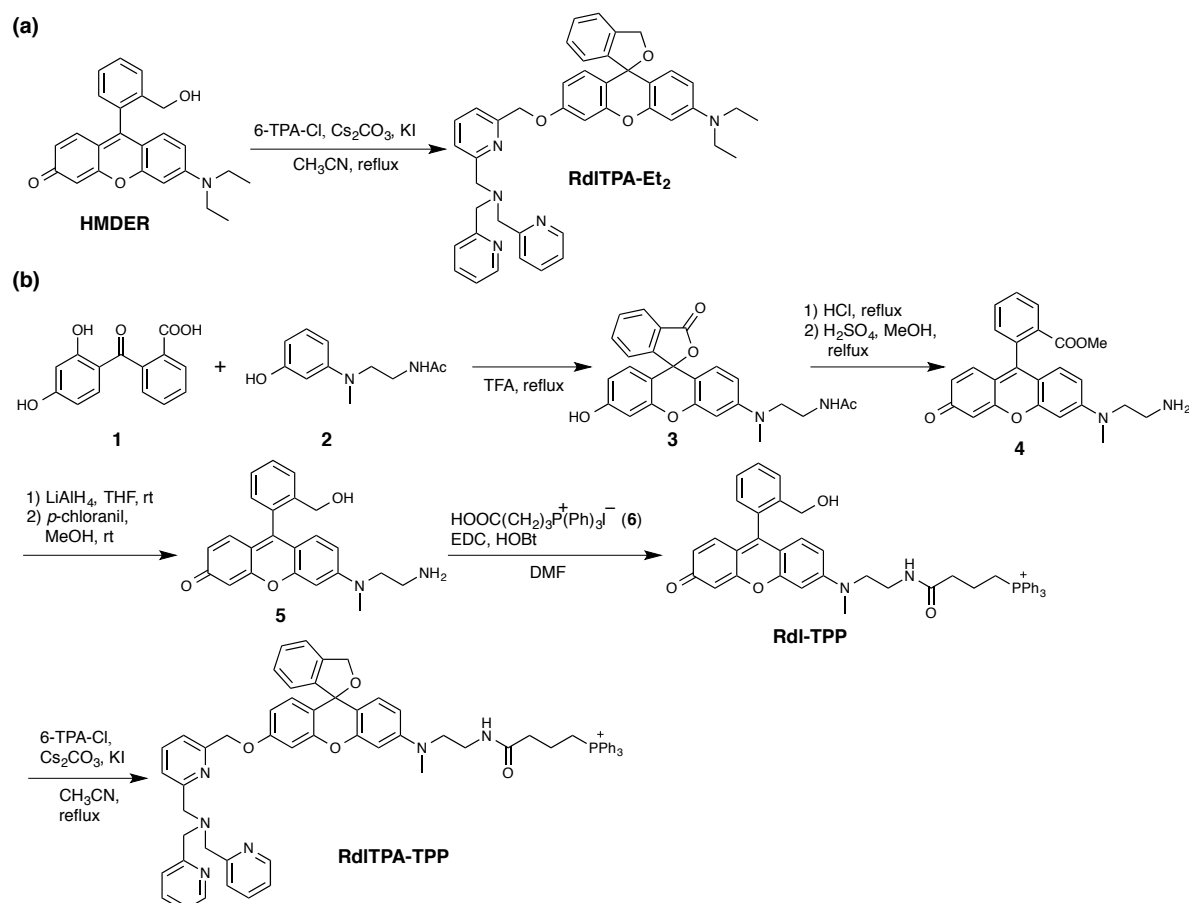


Fig. 1 Fluorogenic probes for Cu^+ based on (a) reduced fluorescein and (b) rhodol platforms.

changes in mitochondrial Cu^+ concentrations to be monitored in living samples. The use of this probe was limited, however, because the small fluorescence on/off ratio (ca. 10-fold) originating in high background fluorescence of the metal-unbound form may often obscure the detection of the desired signals. We have previously reported the development of a reaction-based Cu^+ fluorescent probe (FluTPAs) and its practical application to intracellular Cu^+ imaging.⁶ A reduced fluorescein platform of FluTPAs is essentially non-fluorescent. When copper ions are present in the intracellular reducing environment, C-O bond cleavage of the benzyl ether group followed by air-oxidation results in the formation of a strongly fluorescent compound (Fig. 1a). Although we have succeeded in monitoring intracellular Cu^+ levels in living systems with



Scheme 1 Synthesis of RdITPA-Et₂ and RdITPA-TPP.

FluTPA (R = Me), this probe could not be used to visualize Cu^+ stored in organelles because of the diffusion of not only the probe but also the fluorescent product into cytosol. To address this issue, we have designed a new fluorogenic Cu^+ -selective fluorescent probe bearing an aminoethyl group at the xantheno moiety capable of being modified with an organelle targeting functional group. Hydroxymethyl rhodol, which was recently developed by Urano et al.,⁷ was employed as the fluorophore. When the phenolic hydroxy group of rhodol is alkylated, the equilibrium between the non-fluorescent spirocyclic and fluorescent ring-opened forms should shift to the former of the two forms at the physiological pH of 7.4. According to this fluorescent control mechanism, very little fluorescence should be observed when the phenolic hydroxy group is alkylated with the TPA ligand. Once the TPA moiety has been eliminated by the reaction with Cu^+ , as found in the FluTPA system, the strong fluorescence of the ring-opened form of the rhodol fluorophore should be observed without an additional oxidation step (Fig. 1b). Herein, we describe the synthesis of the TPP-linked Cu^+ -selective fluorescent probe, RdITPA-TPP, and demonstrate the use of this probe for the optical imaging of mitochondrial Cu^+ .

Results and discussion

To evaluate the fundamental fluorescence properties of the rhodol-based Cu^+ probe, we initially prepared RdITPA-Et₂ by the coupling reaction of *N,N*-diethyl rhodol bearing a hydroxymethyl group (HMDER)⁷ with 6-chloromethyl derivative of TPA (6-TPA-Cl),⁸ as shown in Scheme 1a. Any fluorescent impurities were removed by recycling gel permeation chromatography (rec-GPC) prior to its use. All of the spectroscopic measurements of RdITPA-Et₂ were conducted in an aqueous buffer solution (50 mM HEPES, pH 7.20) containing 2 mM GSH, which is the most abundant cellular thiol compound (0.5–10 mM in cells), to simulate the intracellular environment.⁶ RdITPA-Et₂ did not exhibit absorption in the visible region (Fig. S1; see ESI[†]) and had a negligible fluorescence (dotted line in Fig. 2), indicating that the spirocyclic form is the dominant species at neutral pH. When 20 μM of Cu^+ was added to the solution of RdITPA-Et₂ at ambient temperature, a 100-fold increase in the fluorescence was observed (solid line Fig. 2). Analysis of the reaction mixture by HPLC and electrospray ionization mass spectroscopy (Figs. S2 and S3, respectively; see ESI[†]) reveals that HMDER ($\Phi = 0.37$) is generated in almost quantitative

yield (>99%) following a 3 h reaction period. This result indicates that the C-O bond cleavage reaction induced by Cu^+ recognition as demonstrated for FluTPAs proceeds even in the case of the spirocyclized rhodol scaffold.

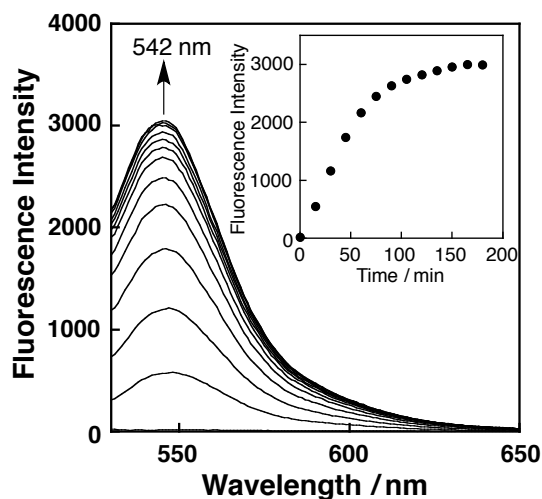


Fig. 2 Fluorescence spectral changes observed upon addition of 20 μM $[\text{Cu}(\text{CH}_3\text{CN})_4]\text{PF}_6$ to the solution of 1 μM RdlTPA-Et₂ in 50 mM HEPES (pH 7.20) containing 2 mM GSH. The spectra were measured every 30 min with the excitation wavelength at 525 nm. Inset: Time course of the fluorescence intensity change at 542 nm.

The fluorescence response of RdlTPA-Et₂ was specific for copper ions (i.e., Cu^+ and Cu^{2+}). Although Co^{2+} caused a relatively small enhancement in the fluorescence (Fig. 3),⁹ this would have little influence in intracellular imaging of Cu^+ because of the existing low level of Co^{2+} *in vivo*. In cells, the oxidation state of the copper ion pool is maintained at +1 with defined redox buffers of glutathione.¹⁰ In fact, no increase was observed in the fluorescence when Cu^{2+} was added in the absence of GSH, which strongly supported the notion that Cu^{2+} is rapidly reduced to Cu^+ under these experimental conditions. Mitochondrial GSH represents approximately 10–15% of the total cellular GSH and the concentration can be as high as 10 mM.¹¹ We confirmed that RdlTPA-Et₂ exhibited detectable fluorescence at concentrations of up to 1 μM of copper ions even in the presence of such high concentrations of GSH (Fig. S4; see ESI[†]). These results demonstrate that the mitochondria-targeting probe RdlTPA-TPP could be applied to monitor the levels of mitochondrial Cu^+ in cells.

The synthesis of RdlTPA-TPP is outlined in Scheme 1b. The benzophenone derivative **1** was synthesized by the decomposition of fluorescein under reflux in a KOH solution.¹² A subsequent Friedel–Crafts reaction between **1** and aminophenol **2**¹³ in boiling TFA afforded the rhodol platform **3**. The deprotection of the *N*-acetyl group in boiling HBr solution, followed by esterification with methanolic sulphuric acid yielded ester **4**, which was then reduced with LiAlH_4 . Subsequent oxidation with *p*-chloranil afforded the rhodol fluorophore **5** bearing a hydroxymethyl group. The coupling reaction between **5** and TPP-carboxylic acid **6** afforded Rdl-TPP, and it is the envisaged fluorescent product

generated by the reaction of RdlTPA-TPP with Cu^+ . The final spirocyclized fluorescent probe was obtained following the alkylation of the phenolic OH group with 6-TPA-Cl and the

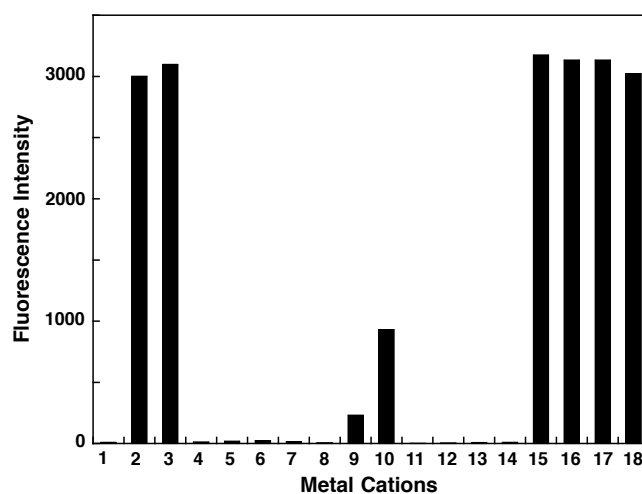


Fig. 3 Fluorescence response of RdlTPA-Et₂ (1 μM) at 542 nm as a function of various added metal cations (5 mM for Na^+ , K^+ , Ca^{2+} , and Mg^{2+} , 20 μM for all other cations) in 50 mM HEPES (pH 7.20). 1, no metal; 2, Cu^+ ; 3, Cu^{2+} ; 4, Na^+ ; 5, K^+ ; 6, Mg^{2+} ; 7, Ca^{2+} ; 8, Mn^{2+} ; 9, Fe^{3+} ; 10, Co^{2+} ; 11, Ni^{2+} ; 12, Zn^{2+} ; 13, Cd^{2+} ; 14, Hg^{2+} ; 15, $\text{Cu}^+ + \text{Na}^+$; 16, $\text{Cu}^+ + \text{K}^+$; 17, $\text{Cu}^+ + \text{Mg}^{2+}$; 18, $\text{Cu}^+ + \text{Ca}^{2+}$.

alkylation of the phenolic OH group with 6-TPA-Cl and the purification of the resulting crude product by HPLC (ODS, $\text{CH}_3\text{CN}/\text{H}_2\text{O}$).¹⁴

Prior to the imaging experiments, the fluorescence of the RdlTPA-TPP towards Cu^+ was confirmed to be comparable to that of RdlTPA-Et₂ (Fig. S5; see ESI[†]). HeLa cells loaded with 10 μM of RdlTPA-TPP exhibited a punctate staining pattern (Fig. 4a and Fig. 4e). To elucidate the stained subcellular localization of the probe, the cells were coincubated with tetramethylrhodamine (TMR) or LysoTracker Red (Fig. 4b and Fig. 4f), which are commercially available fluorescence dyes that can be used for labelling mitochondria or acidic cellular compartments, such as lysosome, respectively. Surprisingly, the micrograph of intracellular RdlTPA-TPP did not colocalize with that of the TMR (Fig. 4c), although it did colocalize well with the LysoTracker Red (Fig. 4g). The spirocyclized structure of RdlTPA-TPP became the ring-opened fluorescent dye at an acidic pH value of ≤ 6 (Fig. S6; see ESI[†]). The probe would therefore exist predominantly in the ring-opened form in the acidic cellular compartments. In contrast, the pH of the MM is 7.8.¹⁵ At this pH, the probe would exist in the spirocyclic form and consequently unable to reveal any fluorescence. For this reason, the presence of the probe in the mitochondria was confirmed using *m*-chlorophenylhydrazine (CCCP), which causes mitochondrial depolarization and uncoupling of respiration. Because the treatment of cells with CCCP induces redistribution of mitochondrially targeted dyes to lysosomal compartments,¹⁶ lysosomal concentration of RdlTPA-TPP should increase, resulting in an increase of fluorescence signals of the ring-opened form. As predicted, an

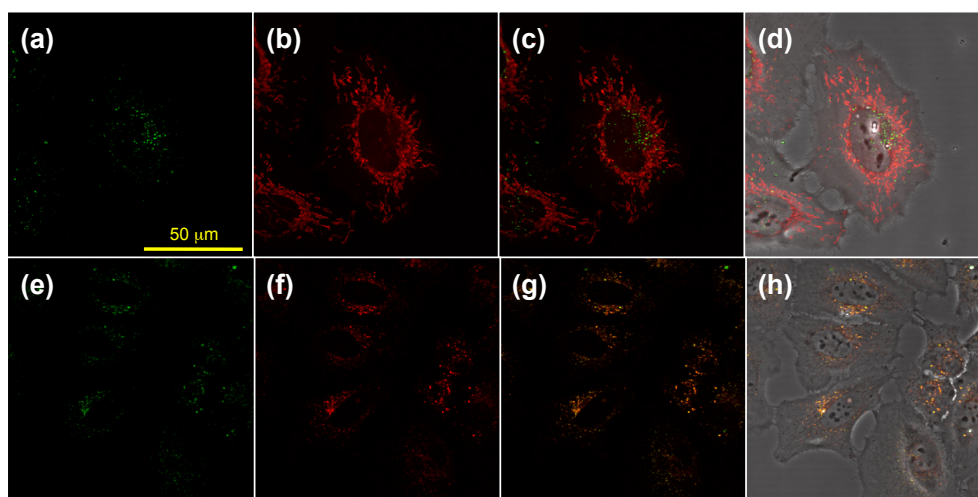


Fig. 4 Localization of RdlTPA-TPP in HeLa cells grown in the basal media. (a-d) Confocal images of the cells loaded with 10 μM RdlTPA-TPP and 75 nM tetramethyl rosamin. (a) RdlTPA-TPP; (b) TMR; (c) overlay of (a) and (b); (d) overlay of bright field image with (c). (e-f) Confocal images of the cells loaded with 10 μM RdlTPA-TPP and 50 nM LysoTracker Red. (e) RdlTPA-TPP; (f) LysoTracker Red; (g) overlay of (e) and (f); (g) overlay of bright field image with (f).

enhancement in the fluorescence of RdlTPA-TPP was observed, although the intensity remained unchanged for LysoTracker Red (Fig. S7; see ESI[†]). This result strongly supports that non-fluorescent spirocyclized probe is certainly localized to mitochondria. Finally, the imaging experiments were then performed with Cu-supplemented HeLa cells, which were grown in DMEM containing 100 μM of CuCl_2 for 6 h at 37 $^\circ\text{C}$. As shown in Fig. 5a, much brighter fluorescence signals compared to those in panels (a) and (e) in Fig. 4 were observed in the cells following 3 h of incubated with 5 μM RdlTPA-TPP. A co-staining experiment with TMR provided a fully merged image that was orange in appearance (Fig. 5b), suggesting that the Cu^+ induced C-O bond cleavage reaction of the probe proceeded to afford a fluorescent product (Rdl-TPP) in the mitochondria. It is noteworthy that a punctate staining pattern derived from the acidic organelle was still visible in Fig. 5b (depicted as green). Given that cells prepared separately that were loaded with Rdl-TPP did not show a similar staining pattern to those described above, it was clear that the probe had not reacted in the lysosome to emit fluorescence.

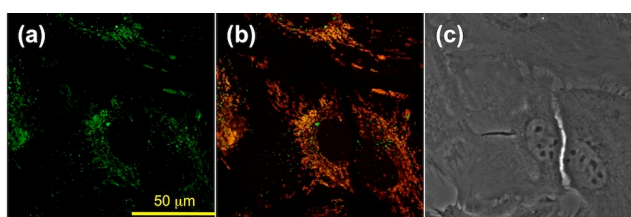


Fig. 5 Detection of mitochondrial copper ion with RdlTPA-TPP. Cu-supplemented HeLa cells were co-incubated with 5 μM RdlTPA-TPP and TMR for 3 h at 37 $^\circ\text{C}$. (a) Fluorescence image of RdlTPA-TPP; (b) merged image of (a) and TMR; (c) brightfield image.

Conclusions

We have developed a new mitochondria-targeted fluorescent probe, RdlTPA-TPP, for detecting Cu^+ . This probe is essentially non-fluorescent at neutral pH because of the spirocyclization of its hydroxymethyl group. The reaction of the probe with Cu^+ under reduction conditions induced the C-O bond cleavage of the benzyl ether, with the resulting cleavage product being simultaneously converted into its fluorescent ring-opened form. Because RdlTPA-TPP needs a long incubation time to generate sufficient fluorescence for detection, this probe is suitable for imaging mitochondrial Cu^+ pools in fluorescence with a high S/N ratio, rather than for the spatiotemporal determination of Cu^+ in living biological samples. The most notable feature of this probe design is the ease with which the subcellular localization of probes can be modulated via the introduction of the different organelle-targeting group instead of the TPP tag. Such organelle specific Cu^+ probes could be used as powerful tools for elucidating the distribution of copper as well as metabolism pathways at a cellular level.

Experimental

Synthesis

General. All chemicals used in this study were commercial products of the highest available purity. 2-(2,4-Dihydroxybenzoyl)benzoic acid (**1**),¹² 3-Hydroxy-*N*-(2-acetamidoethyl)-*N*-methylaniline (**2**),¹³ HMDER,⁷ and 6-TPA-Cl⁸ were prepared according to the reported procedures. NMR spectra were recorded on a JNM-ECX-500 (at 500 MHz to ^1H , 125 MHz to ^{13}C). Chemical shifts are given in ppm relative to tetramethylsilane ($\text{Si}(\text{CH}_3)_4$). HRMS were recorded on a Bruker micrOTOF II (ESI). TLC analyses were performed on Silica gel 60-F₂₅₄ (Merck). Flash chromatography was performed on silica gel (Merck Silica Gel 60). ODS column chromatography was performed on a YFLC system (Yamazen

Co., Osaka, Japan). Recycling preparative HPLC was performed on a LC-9110NEXT system (Japan Analytical Industry Co., Japan) connected to UV detector. Reverse phase HPLC was performed on a Waters Delta 600 system (10 × 250 mm, YMC-Triart C18).

RdlTPA-Et₂. To a solution of HMDER (281 mg, 0.75 mmol), Cs₂CO₃ (688 mg, 2.25 mmol), and KI (125 mg, 0.75 mmol) in dry CH₃CN (50 mL) were slowly added 6-TPA-Cl (254 mg, 0.75 mmol) and the reaction mixture was refluxed overnight under Ar atmosphere. After removal of the insoluble materials by filtration, the filtrate was evaporated. The residue was dissolved in CH₂Cl₂ (100 mL), and the organic layer was washed with water (100 mL × 2) and brine (100 mL), dried over MgSO₄, and concentrated. The crude residue was purified by Al₂O₃ column chromatography (CH₂Cl₂:MeOH = 40:1) to give the title compound as a pale yellow oil (410 mg, 81 %). For spectroscopic analyses, the compound was further purified by preparative HPLC with a linear gradient from 70% solvent A (0.1% TFA in water) and 30% B (0.1% TFA in acetonitrile) to 10% A and 90% B and the collected fraction was lyophilized. ¹H NMR (500 MHz, CDCl₃): δ 1.15 (6H, t, *J* = 6.8 Hz), 3.34 (4H, q, *J* = 6.8 Hz), 3.91 (2H, s), 3.92 (4H, s), 5.19 (2H, s), 5.23 (2H, d, *J* = 3.0 Hz), 6.36-6.40 (2H, m), 6.66 (1H, dd, *J* = 8.8, 2.4 Hz), 6.73 (1H, d, *J* = 8.8 Hz), 6.78, (1H, d, *J* = 2.4 Hz), 6.82 (1H, d, *J* = 8.8 Hz), 6.93 (1H, d, *J* = 8.0 Hz), 7.13 (2H, m), 7.24-7.27 (2H, m), 7.33-7.36 (3H, m), 7.51 (1H, d, *J* = 7.5 Hz), 7.59 (2H, d, *J* = 7.5 Hz), 7.65 (2H, td, *J* = 7.5, 1.5 Hz), 7.67 (1H, t, *J* = 7.5 Hz), 8.54 (2H, ddd, *J* = 5.0, 2.0, 0.5 Hz); ¹³C-NMR (126 MHz, CDCl₃) δ 12.7, 44.6, 60.3, 60.4, 70.9, 71.6, 84.0, 97.8, 101.9, 111.2, 111.6, 118.1, 120.0, 120.7, 121.9, 122.2, 123.2, 124.2, 128.0, 128.3, 129.7, 130.1, 136.6, 137.4, 139.8, 145.0, 148.8, 149.2, 152.1, 152.1, 156.5, 159.0, 159.2, 159.5; MS (ESI pos.) *m/z* calcd for C₄₃H₄₂N₅O₃ ([M+H]⁺) 676.33, found 676.31; calcd for C₄₃H₄₁N₅O₃Na₁ ([M+Na]⁺) 698.31, found 698.29.

Compound 3. A mixture of benzophenone **1** (8 g, 31 mmol) and aminophenol **2** (6.5 g, 31 mmol) in TFA (120 ml) was stirred for 3 h at 95 °C. After cooling to room temperature, TFA was removed by evaporation. The residue was directly purified by SiO₂ column chromatography (CHCl₃: MeOH = 9:1) to give rhodol **3** as a red oil (140 mg, 18 %). ¹H NMR (500 MHz, CD₃OD): δ = 1.83 (3H, s), 3.25 (3H, s), 3.46 (2H, brt), 3.73 (2H, m), 6.86 (1H, dd, *J* = 9.0, 2.5 Hz), 6.98-7.09 (2H, m), 7.07-7.09 (2H, m), 7.36 (1H, d, *J* = 7.5 Hz), 7.79 (1H, t, *J* = 7.5 Hz), 7.84 (1H, t, *J* = 7.5 Hz), 8.28 (1H, d, *J* = 7.5 Hz); ¹³C NMR (500 MHz, CD₃OD): δ = 22.5, 37.9, 39.8, 52.8, 79.4, 98.1, 103.4, 114.7, 115.5, 115.9, 117.7, 129.9, 131.0, 131.5, 132.0, 132.1, 134.4, 139.2, 157.7, 158.6, 158.8, 167.9, 169.0, 174.0; MS (ESI pos.) *m/z* calcd for C₂₅H₂₃N₂O₅ ([M+H]⁺) 431.16, found 431.16.

Compound 4. A solution of rhodol **3** (140 mg, 0.33 mmol) in 1.5 M HCl_{aq} (10 mL) was refluxed overnight. After removal of the solvent, the residue was dissolved in MeOH (50 mL),

followed by addition of conc. H₂SO₄ (0.5 mL). The solution was refluxed for 2 days. After neutralized with NaHCO₃, insoluble inorganic materials were removed by filtration and the filtrate was concentrated in vacuo to yield the ester **4**. The crude was purified by ODS column chromatography eluted with H₂O/CH₃CN (containing 0.1% TFA) to give an orange powder (58 mg, 44 % for 2 steps). ¹H NMR (500 MHz, CD₃OD): δ = 3.28 (2H, t, brt, overlapped with solvent peaks), 3.36 (3H, s), 3.57 (3H, s), 4.01 (2H, brt), 7.02 (1H, dd, *J* = 9.0, 2.5 Hz), 7.20 (1H, d, *J* = 2.5 Hz), 7.25-7.35 (4H, m), 7.43 (1H, d, *J* = 6.5 Hz), 7.81-7.86 (2H, m), 8.32 (1H, d, *J* = 6.5 Hz); ¹³C NMR (500 MHz, CD₃OD): δ = 36.3, 38.9, 49.8, 51.7, 96.9, 102.1, 115.7, 115.8, 116.3, 118.0, 130.1, 130.7, 131.1, 131.6, 132.0, 133.0, 133.4, 157.8, 159.0, 159.1, 163.7, 165.5, 168.9; MS (ESI pos.) *m/z* calcd for C₂₄H₂₂N₂O₄ ([M+H]⁺) 403.17, found 403.17; calcd for C₂₄H₂₂N₂O₄ ([M+Na]⁺) 425.15, found 425.15.

Compound 5. To a solution of compound **4** (50 mg, 0.12 mmol) in dry THF (20 ml) was slowly added LiAlH₄ in small portions at 0 °C until the starting materials were consumed. The mixture was warmed up to room temperature and stirred overnight. 2 M HCl aq was added to the solution until pH became neutral to quench the reaction. The resulting insoluble material was filtrate through a pad of Celite and the filtrate was evaporated in vacuo. The residue was dissolved in dry MeOH (10 mL), followed by addition of *p*-chloranil (89 mg, 0.36 mmol). After stirred for 2 h at room temperature, the solvent was removed and the crude was purified by ODS column chromatography eluted with H₂O/CH₃CN (containing 0.1% TFA) to give an orange powder (28 mg, 63 %).

Rdl-TPP. To a solution of amine **4** (5 mg, 10 μmol) and (3-carboxypropyl)triphenylphosphonium iodide (4.6 mg, 10 μmol) in dry DMF (3 mL) was added EDC (3.8 mg, 20 μmol), DIEA (10 mg, 80 μmol) and HOBt (3.0 mg, 20 μmol). After stirred overnight at room temperature, the solvent was removed and the crude was purified by ODS column chromatography eluted with H₂O/CH₃CN (containing 0.1% TFA) to give an orange powder (2.5 mg, 26 %). Because available amount of this compound was too small for NMR analyses, mass analysis was performed to identify the product. MS (ESI pos.) *m/z* calcd for C₄₅H₄₂N₂O₄P ([M]⁺) 705.28, found 705.28; C₄₅H₄₃N₂O₄P ([M+H]²⁺) 353.15, found 353.14. The overall purity of this compound was also confirmed by HPLC analysis (Fig. S11, see ESI[†]).

RdlTPA-TPP. This compound was prepared according to the synthetic procedure for RdlTPA-Et₂ by using Rdl-TPP instead of HMDER. The final product was ODS column chromatography eluted with H₂O/CH₃CN (containing 0.1% TFA) to give an orange powder (4.7 mg, 80 %). HRMS (ESI pos.) *m/z* calcd for C₄₅H₄₂N₂O₄P ([M]⁺) 1007.441, found 1007.417. The overall purity of this compound was also confirmed by HPLC analysis (Fig. S12, see ESI[†]).

Steady-state absorption and fluorescence spectroscopy

The UV absorption spectra were recorded on a Hewlett-Packard 8453 spectrometer. Fluorescence spectra were recorded using a Hitachi F-2500 spectrometer with a slit width of 2.5 nm. The photomultiplier voltage was 700 V. To reduce the fluctuation in the excitation intensity during measurement, the lamp was kept on for 1 h prior to the experiment. The path length was 1 cm with a cell volume of 3.0 mL. Fluorescence responses of RdITPA-Et₂ to various metal ions were measured as follows. RdITPA-Et₂ (final, 1 μM) was added to 1 mL of HEPES (50 mM, pH 7.20) in the presence of 2 mM GSH. Aqueous solution of transition metal ions (MnCl₂, CoCl₂, NiCl₂, FeCl₃, and ZnCl₂) or [Cu(CH₃CN)₄]PF₆ in CH₃CN was added to give a final concentration of 20 μM. The mixtures were vortexed and kept in dark at room temperature for 3 h. All fluorescence spectra were measured with an excitation wavelength at 525 nm.

Product analysis

To a 1 μM solution of RdITPA-Et₂ in 50 mM HEPES buffer (pH 7.20) containing 2 mM GSH was added a 20 μM solution of [Cu^I(CH₃CN)₄]PF₆ in CH₃CN under aerobic conditions. The mixture was stirred for 3 h at room temperature and analyzed with a reverse phase HPLC (Waters Delta 600 system, 4.6 × 150 mm, YMC-Triart C18) eluted with CH₃CN/H₂O (0.1 % TFA). The retention time was compared with that of an authentic sample HMDER. The yield of the production of HMDER was calculated from the integrated areas of the emission for HMDER to be >99%. For ESI-MS analysis, a 10 μM solution of [Cu^I(CH₃CN)₄]PF₆ in CH₃CN in water was added to a 2 μM solution of RdITPA-Et₂ in 10 mM ammonium acetate containing 100 μM GSH under aerobic conditions. The mixture was stirred for 3 h at room temperature. The samples were directly measured using microTOF II focus (Bruker).

Cell culture experiments

Preparation of cells. HeLa cells were cultured in Dulbecco's modified Eagle's medium (DMEM, Sigma) containing 10% fetal bovine serum (FBS, Gibco) and 1% Antibiotic-Antimycotic (Gibco) at 37 °C in a 5% CO₂/95% air incubator. Two days before imaging, cells (5 × 10⁴) were plated in a 35-mm-diameter glass-bottomed dish and cultured in DMEM. Copper uptake experiments were performed in the same medium except the overnight supplementation of 100 μM CuCl₂ at the end of the incubation period noted above.

Intracellular Localization Analysis. A 5 mM stock solution of RdITPA-TPP in DMSO was diluted to 10 μM in colorless DMEM (without phenol red, Invitrogen). HeLa cells (no copper supplementation) were co-incubated with 10 μM RdITPA-TPP and 75 nM N,N'-tetramethyl rosamine (TMR) or 50 nM LysoTracker Red for 30 min at 37 °C. The cells were rinsed times with colorless DMEM to remove excess probe, and imaged with a FV10i-DOC confocal laser-scanning

microscope (OLYMPUS). The fluorescence images were obtained using corresponding lasers (RdITPA-TPP: λ_{ex} = 473 nm, λ_{em} = 490-540 nm, TMR and LysoTracker Red: λ_{ex} = 559 nm, λ_{em} = 574-674 nm).

Fluorescence imaging of Cu⁺ in cells. Immediately before the staining experiments, Cu-supplemented cells were washed twice with PBS buffer containing 200 μM EDTA to removed extracellular heavy metal ions. A 5 mM stock solution of RdITPA-TPP in DMSO was diluted to 5 μM in colorless DMEM (without phenol red, Invitrogen). The cells were then loaded with RdITPA-TPP (5 μM) and TMR (75 nM) by incubation for 30 min at 37 °C, rinsed three times with colorless DMEM, and imaged under the same conditions described above.

Acknowledgements

This work was financially supported by a Grant-in-Aid for Young Scientists (A) from JSPS (Grant no. 23685039 for M.T.) and the Naito Foundation (M.T.).

Notes and references

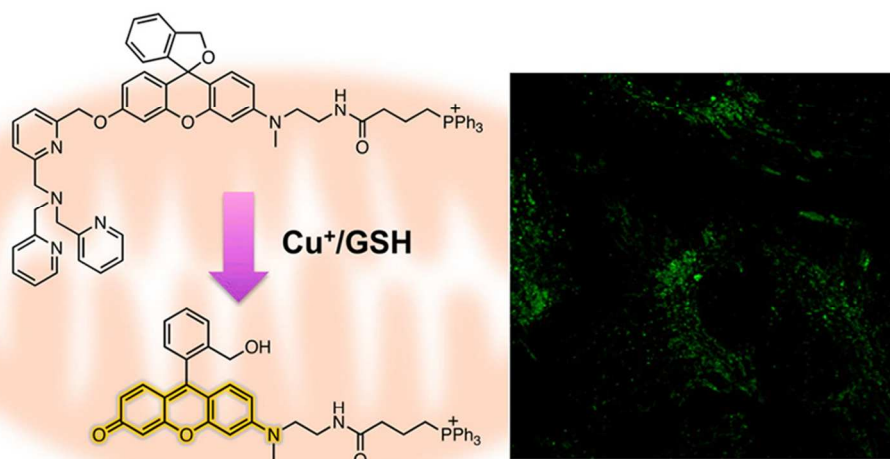
^a Institute of Transformative Bio-Molecules (WPI-ITbM), Nagoya University, Chikusa, Nagoya 464-8602, Japan. E-mail: taki@itbm.nagoya-u.ac.jp

^b Graduate School of Human & Environmental Studies, Kyoto University, Yoshida, Sakyo-ku, Kyoto 606-8501, Japan.

† Supplementary Information (ESI) available: NMR spectra of the new compounds, optical spectra, product analyses, and localization analyses of the probe to cell organelle. See DOI: 10.1039/b000000x/

- 1 C. M. Troy, L. Stefanis, A. Prochiantz, L. A. Greene and M. L. Shelanski, *Proc. Natl. Acad. Sci. U. S. A.*, 1996, **93**, 5635-5640.
- 2 (a) N. J. Robinson and D. R. Winge, in *Annual Review of Biochemistry*, Vol 79, Annual Reviews, Palo Alto, 2010, vol. 79, pp. 537-562; (b) W. L. Pang, A. Kaur, A. V. Ratushny, A. Cvetkovic, S. Kumar, M. Pan, A. P. Arkin, J. D. Aitchison, M. W. W. Adams and N. S. Baliga, *PLoS Comput. Biol.*, 2013, **9**.
- 3 (a) P. A. Cobine, F. Pierrel and D. R. Winge, *Biochim. Biophys. Acta-Mol. Cell Res.*, 2006, **1763**, 759-772; (b) D. L. Huffman and T. V. O'Halloran, *Annu. Rev. Biochem.*, 2001, **70**, 677-701; (c) T. V. O'Halloran and V. C. Culotta, *J. Biol. Chem.*, 2000, **275**, 25057-25060.
- 4 (a) E. L. Que and C. J. Chang, *Chem. Soc. Rev.*, 2010, **39**, 51-60; (b) M. Formica, V. Fusi, L. Giorgi and M. Micheloni, *Coord. Chem. Rev.*, 2012, **256**, 170-192; (c) H. W. Mbatia and S. C. Burdette, *Biochemistry*, 2012, **51**, 7212-7224; (d) Z. P. Liu, W. J. He and Z. J. Guo, *Chem. Soc. Rev.*, 2013, **42**, 1568-1600; (e) L. C. Yang, R. McRae, M. M. Henary, R. Patel, B. Lai, S. Vogt and C. J. Fahrni, *Proc. Natl. Acad. Sci. U. S. A.*, 2005, **102**, 11179-11184; (f) K. A. Price, J. L. Hickey, Z. G. Xiao, A. G. Wedd, S. A. James, J. R. Liddell, P. J. Crouch, A. R. White and P. S. Donnelly, *Chem. Sci.*, 2012, **3**, 2748-2759; (g) A. F. Chaudhry, S. Mandal, K. I. Hardcastle and C. J. Fahrni, *Chem. Sci.*, 2011, **2**, 1016-1024; (h) T.

- Hirayama, G. C. Van de Bittner, L. W. Gray, S. Lutsenko and C. J. Chang, *Proc. Natl. Acad. Sci. U. S. A.*, 2012, **109**, 2228-2233.
- 5 S. C. Dodani, S. C. Leary, P. A. Cobine, D. R. Winge and C. J. Chang, *J. Am. Chem. Soc.*, 2011, **133**, 8606-8616.
- 6 M. Taki, S. Iyoshi, A. Ojida, I. Hamachi and Y. Yamamoto, *J. Am. Chem. Soc.*, 2010, **132**, 5938-5939.
- 7 M. Kamiya, D. Asanuma, E. Kuranaga, A. Takeishi, M. Sakabe, M. Miura, T. Nagano and Y. Urano, *J. Am. Chem. Soc.*, 2011, **133**, 12960-12963.
- 8 V. S. I. Sprakel, J. Elemans, M. C. Feiters, B. Lucchese, K. D. Karlin and R. J. M. Nolte, *Eur. J. Org. Chem.*, 2006, 2281-2295.
- 9 (a) H. Y. Au-Yeung, E. J. New and C. J. Chang, *Chem. Commun.*, 2012, **48**, 5268-5270; (b) D. Maity, V. Kumar and T. Govindaraju, *Org. Lett.*, 2012, **14**, 6008-6011.
- 10 D. W. Domaille, E. L. Que and C. J. Chang, *Nat. Chem. Biol.*, 2008, **4**, 168-175.
- 11 M. Mari, A. Morales, A. Colell, C. Garcia-Ruiz and J. C. Fernández-Checa, *Antioxid. Redox Signal.*, 2009, **11**, 2685-2700.
- 12 M. Inouye, K. Tsuchiya and T. Kitao, *Angew. Chem. Int. Edit.*, 1992, **31**, 204-205.
- 13 T. Hirayama, S. Iyoshi, M. Taki, Y. Maeda and Y. Yamamoto, *Org. Biomol. Chem.*, 2007, **5**, 2040-2045.
- 14 Since available amounts of RdITPA-TPP were too small for $^1\text{H}/^{13}\text{C}$ NMR analyses, the overall purity of the product was confirmed by HPLC and the product was identified by mass analysis (see ESI[†]).
- 15 A. M. Porcelli, A. Ghelli, C. Zanna, P. Pinton, R. Rizzuto and M. Rugolo, *Biochem. Biophys. Res. Commun.*, 2005, **326**, 799-804.
- 16 B. S. Padman, M. Bach, G. Lucarelli, M. Prescott and G. Ramm, *Autophagy*, 2013, **9**, 1862-1875.



80x39mm (300 x 300 DPI)